Sci. Bull. (2016) 61(5):357–367
DOI 10.1007/s11434-016-1028-8

www.scibull.com
www.springer.com/scp

Review

Engineering Sciences

Design and fabrication of 1-D semiconductor nanomaterials for high-performance photovoltaics

Ning Han · Zaixing Yang · Lifan Shen · Hao Lin · Ying Wang · Edwin Y. B. Pun · Yunfa Chen · Johnny C. Ho

Received: 16 December 2015 / Revised: 11 January 2016 / Accepted: 21 January 2016 / Published online: 4 February 2016

Abstract To date, the cost-effective utilization of solar energy by photovoltaics for large-scale deployment remains challenging. Further cost minimization and efficiency maximization, through reduction of material consumption, simplification of device fabrication as well as optimization of device structure and geometry, are required. The usage of 1D nanomaterials is attractive due to the outstanding light coupling effect, the ease of fabrication, and integration with one-dimensional (1-D) semiconductor materials. The light absorption efficiency can be enhanced significantly, and the corresponding light-to-electricity conversion efficiency can be as high as their bulk counterparts. Also, the amount of active materials used can be reduced. This review summarizes the recent development of 1-D nanomaterials for photovoltaic applications, including the anti-reflection, the light absorption, the minority diffusion, and the semiconductor junction properties. With solid progress and prospect shown in the past 10 years, 1-D semiconductor nanomaterials are attractive and promising for the realization of high-efficiency and low-cost solar cells.

Keywords One-dimensional nanomaterials · Photovoltaics · Solar cells · Light absorption · Minority diffusion length · Semiconductor junction

N. Han (✉) · Y. Wang · Y. Chen
State Key Laboratory of Multiphase Complex Systems, Institute of Process Engineering, Chinese Academy of Sciences, Beijing 100190, China
e-mail: nhan@ipe.ac.cn

N. Han · Y. Wang · Y. Chen
CAS Center for Excellence in Urban Atmospheric Environment, Xiamen 361021, China

Z. Yang · H. Lin · J. C. Ho (✉)
Department of Physics and Materials Science, City University of Hong Kong, Hong Kong, China
e-mail: johnnyho@cityu.edu.hk

Z. Yang · L. Shen · E. Y. B. Pun · J. C. Ho
State Key Laboratory of Millimeter Waves, City University of Hong Kong, Hong Kong, China

Z. Yang · H. Lin · J. C. Ho
Shenzhen Research Institute, City University of Hong Kong, Shenzhen 518057, China

L. Shen · E. Y. B. Pun
Department of Electronic Engineering, City University of Hong Kong, Hong Kong, China

1 Introduction

"Historical solar energy" stored in the form of chemical bonds in fossil fuels, such as coal, oil, and so on, are about to exhaust in the next hundred years. More importantly, consumption of these fuels for power generation would emit a lot of hazardous and toxic pollutant gases, such as NO_x, SO_x, and a large amount of greenhouse gas, CO_2, thus threatening the living environment of human beings. Thus, in order to achieve sustainability and create an environmentally friendly human society, abundant and clean energy are essential. In this context, "daily solar energy" is infinite and produces zero-emission, and is believed to be one of the most prospective candidates [1–4]. The solar energy received by earth in 1 h is estimated to be enough for the entire human society consumption for 1 year. However, the utilization efficiency for the natural photosynthesis by green plants is rather low ($\sim$1 %) [1], and consequently, more effective utilization of solar energy has attracted increasing attention all over the world in the form of photovoltaics; by converting sunlight into electricity, solar heat by storing solar energy in water, solar hydrogen production by generating clean fuel, H_2, and so on. Amongst all, the available know-how photovoltaic is the first commercialized technology, and is currently one of the most widely installed and used renewable energies around the world.

Nevertheless, the overall solar energy usage contributes only ~0.1 % to the global energy consumption due to the relatively high monetary energy cost. The energy cost and conversion efficiency of different kinds of photovoltaic materials and technologies are summarized in Fig. 1 [1]. For the first generation of single crystalline silicon based solar panels, the efficiency approaches the Shockley–Queisser limit and reaches around 20 %, but the material synthesis, the cell integration, and the packaging and transportation still contribute a significant part of the overall cost, thus they are not cost attractive for terrestrial use. For the second generation of thin film based solar cells, the aims are to lower the overall costs and increase the cost effectiveness by having a moderate efficiency while reducing the high material costs. However, this approach still suffers from relatively high cost (5–10 folds) as compared with traditional fuel-electricity or water-electricity. In this regard, for the third generation of photovoltaics the aims are to achieve higher efficiency as well as lower production cost in order to be price competitive. In general, the ultimate solar cell efficiency has its theoretical limit known as the Shockley–Queisser or the thermodynamic limit, which restricts the cost effectiveness by capping the cell efficiency. Due to the recent advent of nanotechnology, the energy cost effectiveness of photovoltaics can be greatly increased by using nanostructured materials, the material consumption in the cell fabrication process and hence the cost is reduced. As a result, nanostructured materials especially 1-dimensional (1-D) nanowires (NWs) are widely adopted as both the active junction materials and the anti-reflection layers, and high-efficiency and low-cost photovoltaics are obtained.

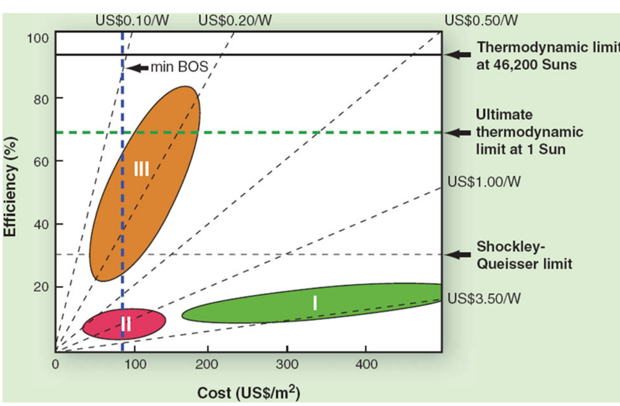

Fig. 1 (Color online) Comparison of different photovoltaic technologies with respect to both the cost and efficiency. The Shockley–Queisser limit is based on single-junction photovoltaics which is ~30 % as photons with energy lower than the bandgap will not be absorbed while those with higher energy will thermalize. However, if this extra energy can be fully utilized to generate electricity rather than thermally lost, the efficiency would increase to ~70 % giving the thermodynamic limit. Reprinted with permission from Ref. [1]

Also, there is a need for special and portable power sources, such as flexible and wearable solar cells for clothing, transparent cells for smart phones and self-powered windows, and so forth [5, 6]. Conventional rigid Si panels and thin film devices cannot serve as the active cell materials in these cases, because they are neither flexible to be compatible with bending, nor transparent to be adopted for see through applications. Hence, highly-efficient and low-weight NW based solar cells is an ideal candidate for these smart flexible power supplies, since the nanomaterials can alleviate mechanical strain easily and absorb and transmit sufficient sunlight when put on glasses [7]. 1-D nanomaterials are attractive and promising for terrestrial photovoltaics and smart flexible power sources, because of their efficient coupling with sunlight and effective light-to-electricity conversion capabilities, as detailed in the following sections. The synthesis of 1-D semiconductor nanomaterials are well overviewed in Refs. [8–11], hence they will not emphasized herein and will be incorporated into different sections where they are mentioned. Similarly, many articles have been written on the design and fabrication of photovoltaic devices (Refs. [12–16]). Therefore, we dedicate this review to the challenge, design and fabrication of NWs-based photovoltaics emphasizing on important parameters such as light scattering and absorption, electron/hole generation, and separation and collection by the device junctions.

2 Light scattering and absorption properties of 1-D nanomaterials

Solid material absorbs incident light, and according to the Lambert–Bill law the absorption A can be written as $A = kd$ where k is a constant, and d is the material thickness. Hence, photovoltaic cells should have enough active material thickness for effective absorption of sunlight. However, this is based on ray optics with the assumption that the absorber has a much larger dimension than the wavelength of incident light. For nanostructured materials with dimensions comparable with or smaller than the wavelength of incident light, resonance will occur and ray optics is no longer valid. The light absorption area is enhanced and the physical cross-sectional projected area is greatly increased [17, 18]. Besides the dimension, other factors such as crystal phase and orientation will also significantly affect the resonance absorption efficiency [19]. For example, Heiss and Morral [20] have simulated the light absorption of a horizontal nanowire lying flat down on a substrate as shown in Fig. 2a–c. External quantum efficiency (EQE) refers to the efficiency calculated based on all the incident sunlight or photon, while the internal quantum efficiency (IQE) designates the efficiency based on the already absorbed sunlight. As a result of the built-in light concentration by Mie resonances, the absorption cross-section can be significantly larger than the physical cross-section of the nanowire. The simulated EQE/IQE ratio can be as high as 1, showing that the light absorption of NWs can be effective and comparable with their thin film counterparts. Furthermore, if the NWs are arranged in two dimension array form in the wavelength scale, the light absorption area can be 10 times as large as their projected area [21]. This enhanced light absorption area enables vertical standing NWs based photovoltaics having an efficiency of up to 40 %, based on the projected area as depicted in Fig. 2d–f. Even though the resonance absorption is limited by the NWs arrays, a large amount of material consumption is reduced due to the light concentration effect, and the efficiency is improved further under concentrated solar field. And recently, there are also some simulations showing the GaAs NW solar cells have the efficiency limit of ~42 % [22], and InP NW array solar cells have up to 32.5 % efficiency [23]. Therefore, nanostructured materials are advantageous in absorbing sunlight in a cost-effective manner, and their potentials in increasing the photovoltaic cost effectiveness and reducing the electricity production cost are demonstrated.

1-D nanostructures also exhibit distinguished anti-reflection and light trapping effect, the light is scattered back and forth and the light absorption depth is increased [24–28]. This kind of anti-reflection layer is essential in maximizing the absorption of incident sunlight, and is extremely important for thin film photovoltaics since the typical active cell material thickness is in the micrometer scale only; this thickness is normally considered too thin for sufficient photon absorption. Recently, Fan's group have developed various kinds of structures, such as nanocones, nanospikes, integrated nanopillars, and nanowells, on aluminum via anodic oxidation technology, in order to minimize the optical reflection to below 5 % [29–32]. Likewise, we have also designed and developed different types of 1-D Si nanostructures, such as nanopillars, nanorods, nanopencils, nanocones, and others by wet chemical etching method, with an aim to integrate active cell structures with anti-reflection functionality [33, 34]. As shown in Fig. 3, the simulation and the experimental results confirm that the well-developed nanopencil arrays are the most

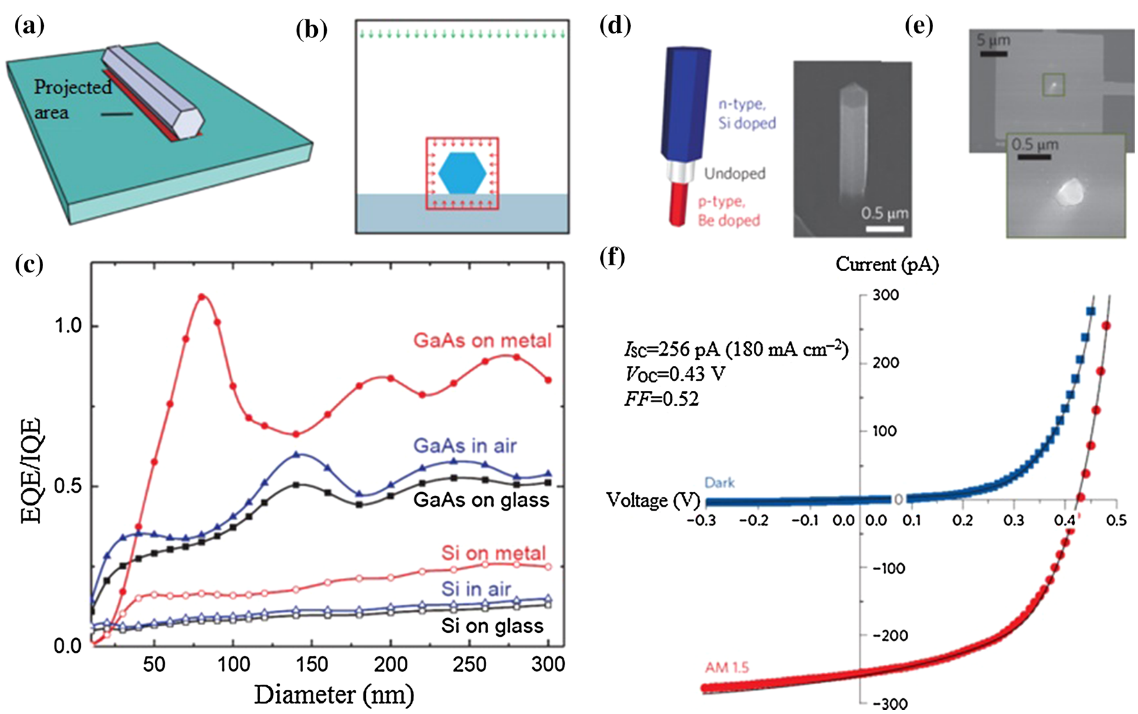

Fig. 2 (Color online) Simulation and experimental results of light absorption of a horizontal nanowire lying down on a substrate. **a, b** The NW simulation details; **c** The EQE/IQE ratio of GaAs and Si NWs; **d** Schematic and SEM image of a GaAs NW; **e** SEM image of the NW seen from the top; **f** the *I*–*V* characteristic of a representative single NW photovoltaic cell. Reprinted with permission from Refs. [20, 21]

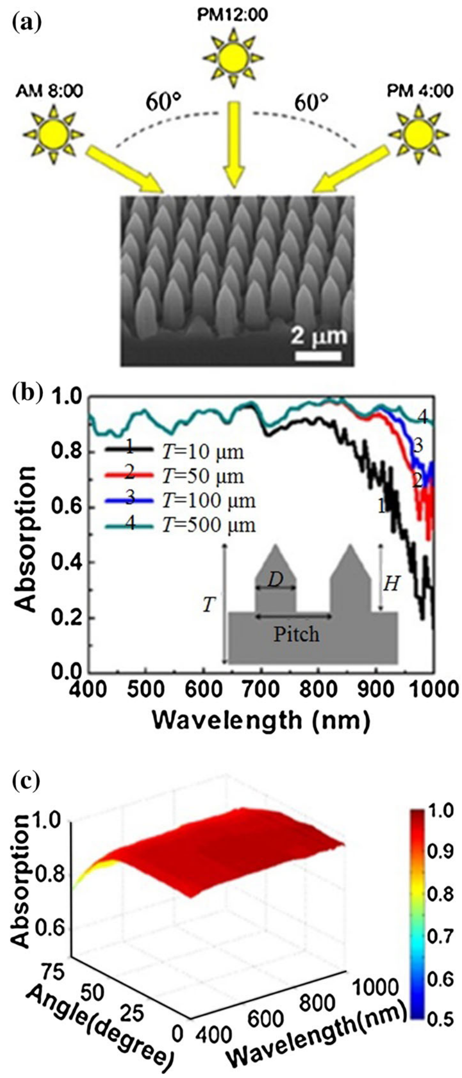

Fig. 3 (Color online) Si nanopencil anti-reflection layer. **a** SEM image demonstrating the omni-directional light absorption property; **b** Absorption characteristics of the nanopencil arrays with different substrate thickness; **c** The angle and wavelength dependent absorption behavior. Reprinted with permission from Ref. [33]

effective approach in absorbing sunlight with omnidirectional performance, and similar results have also been observed for tapered InP NW arrays with inverted nanopencil structure [35] and dual diameter nanopillar arrays [36]. All these results illustrate and confirm the advantages of using 1-D nanostructures in light trapping engineering, especially for active cell structures integrated with anti-reflection properties [37].

3 Material design and synthesis for long minority diffusion length

In general, after sunlight is absorbed by semiconductor the phonons will excite electrons from the valence band (E_v) to the conduction band (E_c). The phonon generated electron/hole pair is not stable but should have a long enough lifetime (τ) to be effectively collected by the built-in potential in the p-n junction. In this case, the time-resolved photoluminescence is a versatile technology in determining the minority lifetime, and a lifetime in the range of picoseconds (ps) to nanoseconds (ns) is usually measured for NW materials [38–42]. For example, Zhang et al. [43] recently observed that the carrier lifetimes of intrinsic and sulfur-doped InP Nanowires are 200–300 and 2–40 ps respectively. A more direct parameter is the diffusion length L of the minority carriers, which determines the ultimate collection of photon induced electron/hole pair. Based on the equation: $L = (\mu\tau kT/e)^{1/2}$, where μ is the mobility and kT/e is a constant, L depends strongly on the minority carrier properties and is a combination of both the mobility and the lifetime [44, 45]. The diffusion length can be directly measured by electron-beam induced current (EBIC) method as detailed in Fig. 4, according to the formula $I_{EBIC} \propto I_0 \exp(x/L_D)$. The measured results of the diffusion length are in good agreement with the calculated results, with a typical value ~150 nm for GaAs NW [44]. Thus, τ or L is one of the key factors in determining the overall efficiency of photovoltaic cell, and effective design should focus on eliminating the recombination center of the electron/hole, such as crystal defect, dopant, surface state, and so on. For nanomaterial, crystal defect easily exists owing to the thermodynamically comparable crystal phase and plane, and surface state is abundant because of the extraordinarily large surface-to-volume ratio of NWs with unbounded surface atom as compared with the bulk counterpart [46, 47]. Hence, controlling the crystal defect and the surface state are one of the major challenges in developing highly-efficiency nanowire based photovoltaics.

There are several ways to reduce the crystal defects of semiconductor NWs. Joyce et al. [48] and Krogstrup et al. [49] found that by tuning the V/III ratio and the growth temperature, phase-pure III–V NWs with minimized defects can be obtained. They also reported that by providing more active precursors for faster growth rate, the NWs grown will have better crystallinity [50]. Steffen et al. [51] found that self-catalyzed GaAs NWs have longer minority carrier lifetime as compared with Au catalyzed ones, probably due to the lower Au residual atom recombination centers, which most likely are located in the crystal defect sites [52]. In our previous studies, we found that by improving the supersaturation of Au–Ga alloy, the NWs grown will have better crystallinity due to the higher driven force for the NW growth [53, 54]. This supersaturation effect is also effective in other material systems, such as InAs NWs as reported by Zhang et al. [55], and Ge NWs grown by O'Regan et al. [56, 57] All these results show that different growth optimization schemes are all

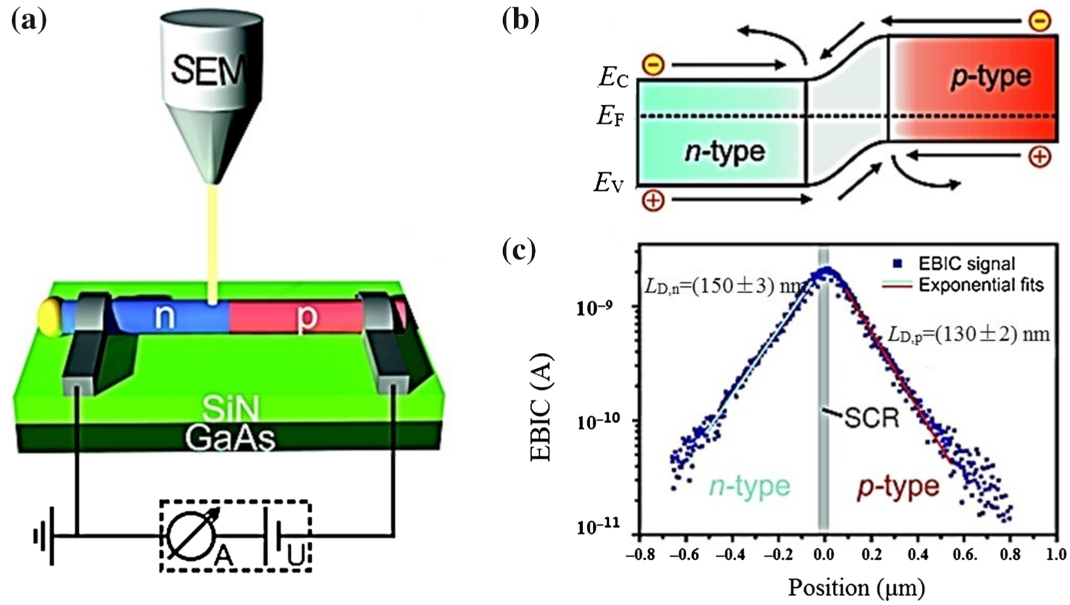

Fig. 4 (Color online) Schematics and measurement results of electron-beam induced current (EBIC) mapping for the determination of minority carrier diffusion length. **a** Measurement schematic and mechanism; **b** Corresponding band diagram of the nanowire during the measurement; **c** Diffusion length of hole ($L_{D,p}$) and electron ($L_{D,n}$) measured in the n- and p-doped nanowire segments. Reprinted with permission from Ref. [44]

effective in reducing the crystal defects and obtaining highly crystalline semiconductor nanomaterials.

The surface states can be reduced significantly by two methods. One is the post-growth sulfide passivation method [58], and the other one is the in situ inert shell fabrication [59]. Tajik et al. [60] found that GaAs surface states can be effectively reduced by post-growth ammonia sulfide $(NH_4)_2S_x$ passivation, and the photovoltaic efficiency can be greatly enhanced. In recent years, the in situ shell growth is commonly adopted and proven to be very effective. For example, Mariani et al. [61] found that an InGaP shell layer can effectively alleviate the surface states of GaAs NWs, enhancing the corresponding device performance as shown in Fig. 5a–d. Kelzenberg et al. [63] also found that surface passivation of Si wires using a-Si or SiN can increase the minority carrier diffusion length L by up to and longer than 30 μm, and with low surface recombination velocity. In our previous study, we have developed an in situ sulfur passivation method [62] for the reduction of surface-states of GaSb and GaAs, and an record hole mobility of 200 cm^2/(V s) has been obtained for ~30 nm diameter GaSb nanowires as illustrated in Fig. 5e, f.

4 Junction design for efficient carrier separation

Long carrier lifetime or diffusion length can only provide the probability of generating photovoltaic electricity; the other required important parameter is high junction barrier height in order to drive the photo-induced electron/hole separation and collection. For further optimization with high flexibility in the structural design, conventional p-i-n junction and metal–insulator-semiconductor (MIS) Schottky barrier configurations can also be fabricated in nanomaterials [64, 65]. For example, the i-layer can be specifically designed to reduce junction current leakage. Holm et al. [66] fabricated a radial p-i-n junction GaAsP NW solar cell with InGaP as the passivation layer, and the cell exhibit an impressive high efficiency of 10 %. Typical axial p-i-n junction along a single Si nanowire and its photovoltaic performance are shown in Fig. 6a, b [64]. Adopting the p-InP substrate as the back contact and transparent conductive oxide (TCO) as the top transparent electrode, the NW arrayed solar cell yields a record high efficiency of 13.8 % with only ~12 % coverage of the NWs on the surface [67]. There are also other promising junction designs, such as the three-dimensional (3D) p-n junctioned CdS/CdTe photovoltaic devices which yield high efficiency of ~6 % on flexible substrates, as illustrated in Fig. 6c, d [7]. The unique advantage of radial junction structured solar cells is the orthogonal direction of light absorption versus carrier collection, the photocurrent is harvested more effectively and thus higher efficiency can be achieved.

On the other hand, NWs based metal–semiconductor Schottky barrier solar cells cannot provide the same high energy conversion efficiency as compared with junction structures. The main problem is that the well-known

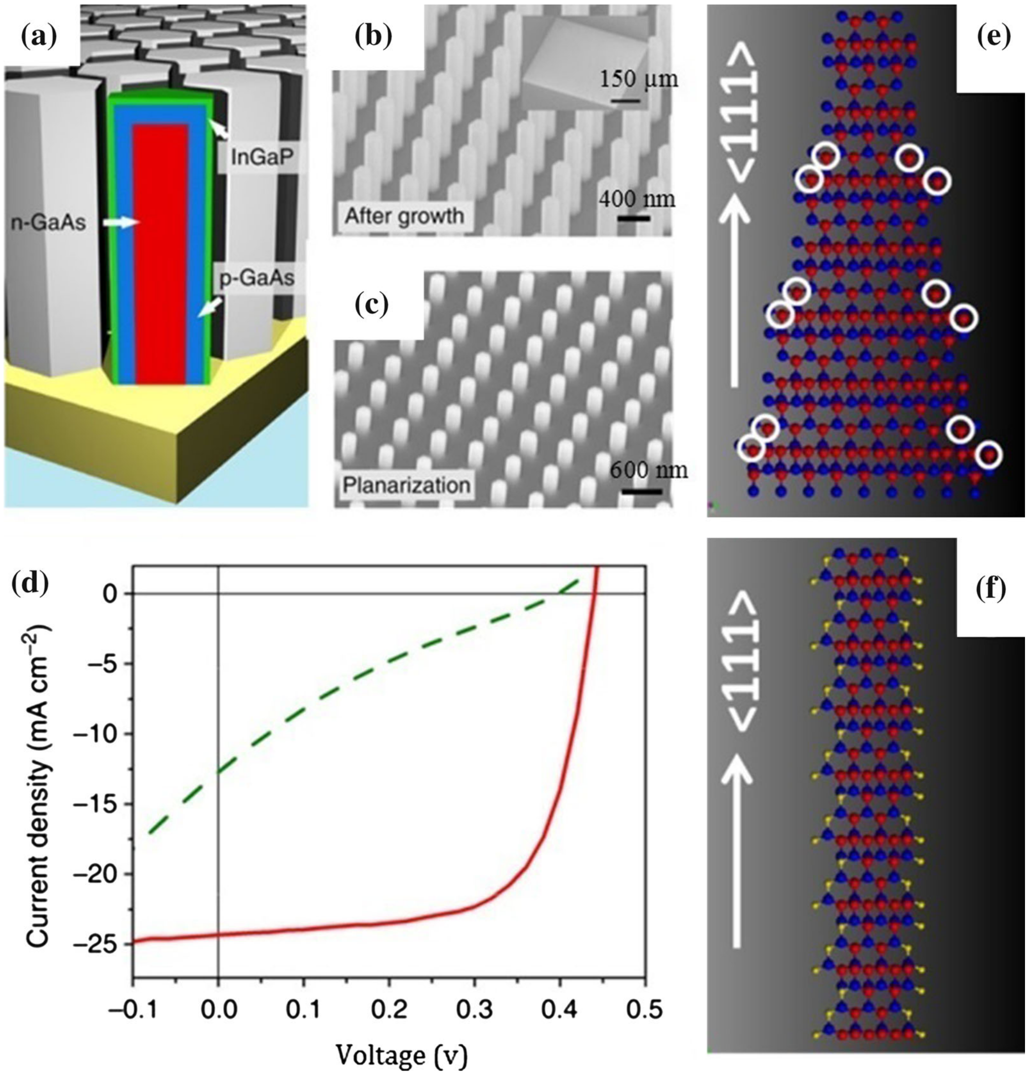

Fig. 5 (Color online) In-situ surface passivation of III–V NWs. **a** Schematics of the GaAs radial p-n junction with InGaP passivation layer; **b**, **c** SEM images of the GaAs NW arrays; **d** IV curves of the cell with and without the InGaP passivation; **e**, **f** In-situ sulfur surface passivation schematics of the GaSb and GaAs NWs. Reprinted with permission from Refs. [61, 62]

surface Fermi-level pinning, resulting from the abundant surface states of the high surface-to-volume ratio nanomaterials, hampers the effective device design and the fabrication of high Schottky barriers [68, 69]. This Fermi-level pinning is extremely severe in III–V compound semiconductors with high concentrations of surface states. For example, InAs NWs always have their surface Fermi-level pinned above the conduction band edge, which can only be eliminated by the novel design of InAs/InP core/shell structure [70]. In our previous study [71], we have also found that the Schottky barrier height is rather low for thermally deposited Ni-Au electrode contacts, and the open circuit voltage (V_{oc}) of the fabricated NW device is as low as $\sim$0.1 V. However, when we have employed Au/Ga catalyst tip as the Schottky electrode and used thermally deposited Ni as the Ohmic electrode, a much higher V_{oc} of $\sim$0.6 V has been obtained, as illustrated in Fig. 7a–d. This high V_{oc} corresponds well with the Schottky barrier estimation of Au/GaAs with Fermi levels of $\sim$5.3 and 4.8 eV, and is attributed to the atomic connection of the Au catalyst with the GaAs NW body without any surface/interface states. Moreover, the radial Schottky barrier has also been fabricated by Ye et al. [72] for CdS/Au core/shell structures. Although the short circuit current (I_{sc}) is high, the V_{oc} is still relatively low due to the unavoidable Fermi-level pinning. It should be noted that Schottky barrier solar cells have comparable high theoretical efficiency but lower cost due to its ease of fabrication as compared with the complicated and complex p-i-n junction structures. Therefore, it is a technological challenge and offers good opportunity for researchers

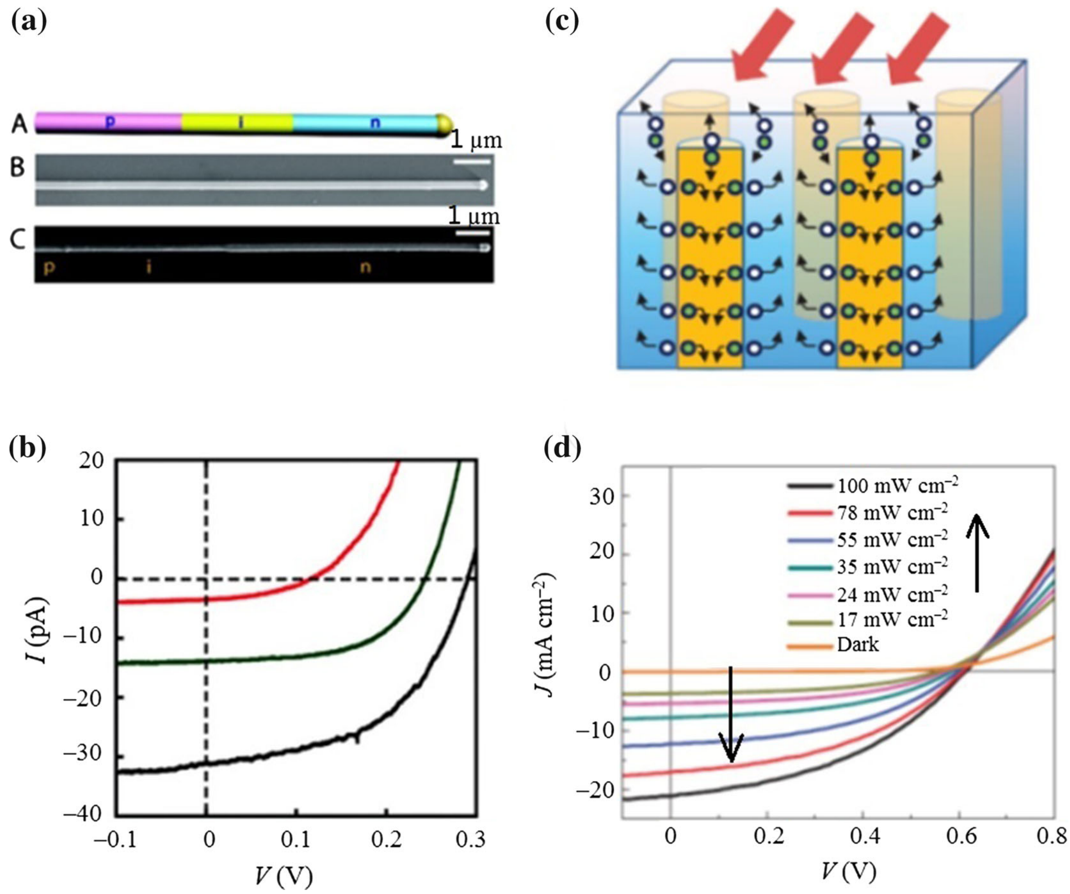

Fig. 6 (Color online) Axial and radial NW junctions. **a** Schematic and SEM images of the Si NW axial p-i-n junction; **b** Light *I*–*V* characteristics of p-i-n Si NW photovoltaic devices with different i-region lengths. The upper, middle and bottom curves (red, green, and black curves online) correspond to i-segment lengths of 0, 2, and 4 μm, respectively; **c** schematics of the CdS/CdTe NW 3-D radial junction solar cells; **d** The *I*–*V* curves of the cells under different illumination intensities. Reprinted with permission from Refs. [7, 64]

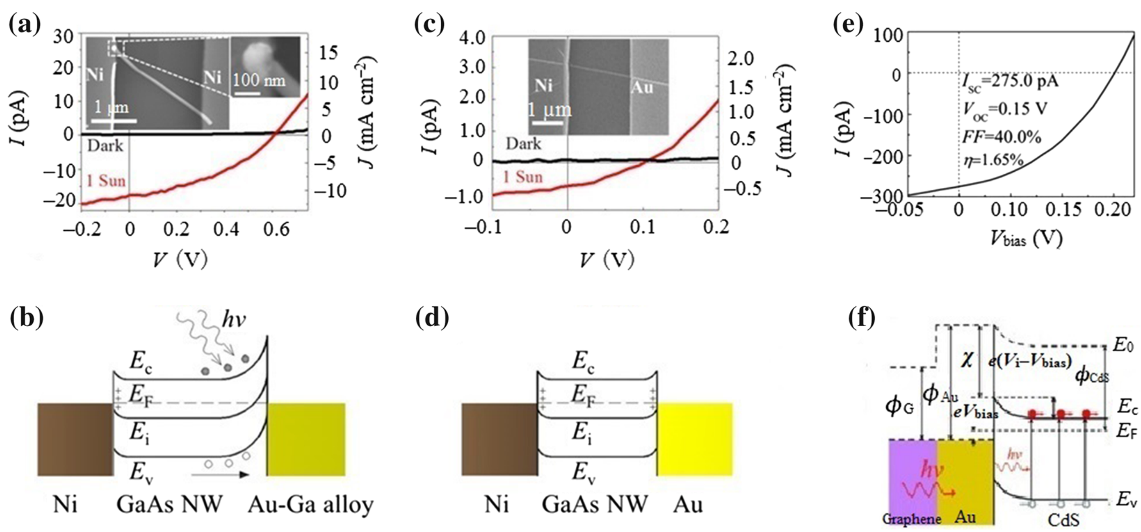

Fig. 7 (Color online) Schottky barrier single NW photovoltaic devices. **a**, **b** SEM image and *I*–*V* curve of the AuGa catalyst/GaAs NW body Schottky contact solar cell and the corresponding band diagram; **c**, **d** SEM image and *I*–*V* curve of the thermally deposited Au Schottky barrier NW solar cell and the corresponding band diagram; **e**, **f** *I*–*V* curve and band diagram of the CdS/Au core/shell Schottky barrier NW solar cell. Reprinted with permission from Refs. [71, 72]

to attempt realizing Schottky contact on nanomaterials for high-efficiency and low-cost photovoltaics.

The versatility of NW structure designs can also facilitate the reinforcement of solar cell outputs. As shown in Fig. 8a, b, the p-i-n/p-i-n tandem structure can be easily fabricated using individual Si NW by tailoring the growth parameter, and thus the V_{oc} of this structure can have a two-folds increase as compared with single junction ones [64]. Similar results have also been obtained using InP NWs [74]. Output enlargement is also attained for Schottky barrier photovoltaics [73, 75]. Yang et al. [73] reported using a Sc/Pd asymmetric Schottky contact, and carbon nanotube based photovoltaics have been easily obtained with higher V_{oc} by tailoring the number of tandem electrode pairs. All these milestone and excellent results confirm the promising prospect of NW based high efficiency and low-cost.

5 Summary of NW photovoltaic performance

1-D semiconductor nanomaterial based photovoltaics have been extensively explored from the late 2000, with pioneering works from Lieber's, Atwater's, Lee's, Yang's groups, and so on. Initially, single Si NW based photovoltaic device has an efficiency of 0.5 %–3.4 % only [64, 76–79], but the efficiency is now routinely increased to 5 %–10 %. Excellent work by Krogstrup et al. [21] reported an apparent efficiency of ~40 % beyond the Shockley–Queisser limit. This is due to the efficient light coupling effect of the NWs having diameters in the range of the wavelength of incident photon. It should be noted that single NW output is relatively low due to the small active absorption area as compared with its thin film counterpart, and the light concentrating effect is also limited. However, the advantages of lower material consumption and the unique configuration of NW arrayed cells are very attractive and promising for realizing high-efficiency and low-cost solar devices, such as the ones demonstrated in Figs. 4, 5. The overall progress of 1-D NW based photovoltaics is summarized in Table 1, and the milestones in the development of NW based solar cells towards cost-effectiveness and smart power supplies can be seen easily.

Besides the benefit of lower material consumption by employing NWs there are other merits, for example, 1-D NWs can be grown on non-crystalline substrates such as SiO_2, glass, and so on [82], which can further reduce the material production cost as compared with epitaxial growth of crystalline thin films. Dhaka et al. [82] have synthesized GaAs NWs on glass substrates with high growth rate and high yield. We have also prepared GaAs NWs on SiO_2 substrates using solid-source chemical vapor deposition method, and the high-quality NWs have also been utilized for effective Schottky barrier solar cells [71, 83]. Hence, all

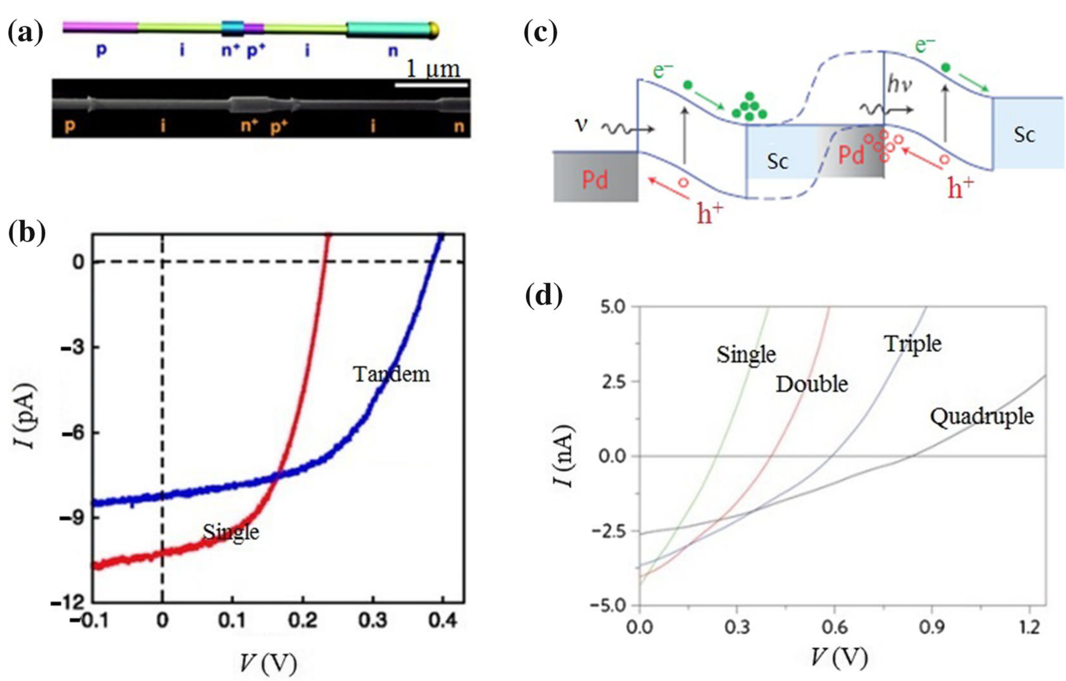

Fig. 8 (Color online) Multiplication of the NW photovoltaic output. **a**, **b** Schematic and *I–V* curves of single Si NW p-i-n/p-i-n junction photovoltaic devices; **c**, **d** band diagram and *I–V* curves of the Pd/Sc asymmetric contacted carbon nanotube solar cells. Reprinted with permission from Refs. [64, 73]

Table 1 Performance summary of nanowire based photovoltaics

Material	Growth	Junction	Passivation	Efficiency[a]	Ref.
Si	CVD	Radial p-i-n	a-Si, SiN	9 % for single horizontal wire, 17 % for vertical array	[63]
Si	CVD	Radial p-i-n	NA	6 % for single, and 15 % for 5-stack horizontal wires	[17]
GaAs	MBE	Radial p-i-n	NA	4.5 % horizontal single NW	[80]
InP	MOVPE	Axial p-i-n	NA	5 % horizontal single NW	[74]
CdS/Cu_2S	Solution	Radial p-i-n	NA	5.4 % horizontal single NW	[81]
GaAsP	MBE	Radial p-n	InGaP	10.2 % horizontal single NW	[66]
GaAs	MBE	Radial p-i-n	NA	40 % vertical single NW	[21]
GaAs	CVD	Schottky barrier	NA	16 % for horizontal single NW	[75]
Si	RIE	Radial p-n	NA	5.3 % vertical array	[27]
GaAs	MOCVD	Radial p-i-n	$(NH_4)_2S$	2.54 % vertical array	[58]
GaAs	MOVPE	Radial p-i-n	InGaP	6.63 % vertical array	[61]
InP	MOCVD	Axial p-i-n	NA	13.8 % vertical array	[67]

[a] The efficiency of single NW PV is based on the active projected NW area rather than the physical light absorption area, and thus the efficiency is referred to as apparent efficiency

these low-material production together with the simple and successful cell fabrication advantages show promises in the utilization of NWs for third-generation photovoltaic devices.

6 Conclusions and perspectives

In summary, 1D semiconductor nanomaterials for photovoltaic applications have been demonstrated with many promising advantages, such as lower material consumption and high photon-to-electricity conversion efficiency. The high efficiency is not only due to the effective light trapping and antireflection properties making full use of the incident sunlight, but also owing to the light concentrating effect of much larger photon absorption area as compared with their physical projected cross-sectional area. All these have been demonstrated with representative GaAs NW device with an apparent efficiency of 40 % beyond the Shockley-Queisser limit, and this high efficiency can be attributed to the resonant absorption of NW with diameter in the incident light wavelength range. Many challenges still exist due to the high surface-to-volume ratio of nanomaterials, such as the high concentration of recombination centers (e.g. crystal defect and surface state), which can shorten the minority carrier lifetime and the diffusion length. Also, the surface Fermi-level pining makes the fabrication of efficient NW junction difficult. Despite all these difficulties, high efficiency single NW photovoltaic devices have been fabricated, and InP nanowire arrayed solar cells with an efficiency of up to 13.8 % have been realized, and this efficiency is comparable with the thin film counterparts. Thus, significant progresses have been made in employing NWs as active device materials towards the third generation high-efficiency and low-cost photovoltaics.

Recently, many other advanced technologies have also emerged that can further enhance the NW based photovoltaic performances, such as incorporating Au nanoparticles to realize surface plasmon enhanced solar cells [84–86], hot electron separation and collection [87–89], realizing multiple-exciton generation [90], as well as multi-terminal NW solar cells [91]. Moreover, in order to eliminate the utilization of rare earth elements in III–V semiconductors, low-cost oxide-based photovoltaic devices are also being actively pursued. Even though at present the measured efficiency is low, in the order of 0.05 %–0.5 % due to the unsuitable bandgap and low carrier mobility (i.e. short diffusion length) [92, 93], there are potentials for substantial improvement in the near future. Although photovoltaics always suffer from the shortcoming of fluctuation of sunlight with time and altitude, this can be overcome by complementary development of energy storage technologies such as batteries, and so on. In battery applications, using 1-D nanomaterials can also plays a key role in improving the energy storage capacity. Therefore, the 1-D semiconductor nanomaterials are attractive and promising active materials for improving solar energy conversion and storage, alleviating the problems of energy crisis, and contributing to green technology and well-being of mankind.

Acknowledgments This work was supported by the Early Career Scheme of the Research Grants Council of Hong Kong SAR, China (CityU 139413), the National Natural Science Foundation of China (51202205 and 61504151), the State Key Laboratory of Multiphase Complex Systems (MPCS-2014-C-01 and MPCS-2015-A-04), the

Science Technology and Innovation Committee of Shenzhen Municipality (JCYJ20140419115507588), and a Grant from the Shenzhen Research Institute, City University of Hong Kong.

Conflict of interest The authors declare that they have no conflict of interest.

References

1. Lewis NS (2007) Toward cost-effective solar energy use. Science 315:798–801
2. Service RF (2005) Is it time to shoot for the Sun? Science 309:548–551
3. Crabtree GW, Lewis NS (2007) Solar energy conversion. Phys Today 60:37–42
4. Han X, Xu C, Ju X et al (2015) Energy analysis of a hybrid solar concentrating photovoltaic/concentrating solar power (CPV/CSP) system. Sci Bull 60:460–469
5. Schubert MB, Werner JH (2006) Flexible solar cells for clothing. Mater Today 9:42–50
6. Lunt RR, Bulovic V (2011) Transparent, near-infrared organic photovoltaic solar cells for window and energy-scavenging applications. Appl Phys Lett 98:113305
7. Fan ZY, Razavi H, Do JW et al (2009) Three-dimensional nanopillar-array photovoltaics on low-cost and flexible substrates. Nat Mater 8:648–653
8. Dick KA (2008) A review of nanowire growth promoted by alloys and non-alloying elements with emphasis on Au-assisted III–V nanowires. Prog Cryst Growth Charact Mater 54:138–173
9. Fang M, Han N, Wang F et al (2014) III–V nanowires: synthesis, property manipulations and devices applications. J Nanomater 2014:702859
10. Wacaser BA, Dick KA, Johansson J et al (2009) Preferential interface nucleation: an expansion of the VLS growth mechanism for nanowires. Adv Mater 21:153–165
11. Yu R, Lin QF, Leung SF et al (2012) Nanomaterials and nanostructures for efficient light absorption and photovoltaics. Nano Energy 1:57–72
12. LaPierre RR, Chia ACE, Gibson SJ et al (2013) III–V nanowire photovoltaics: review of design for high efficiency. Phys Status Solidi RRL 7:815–830
13. Lunt RR, Osedach TP, Brown PR et al (2011) Practical roadmap and limits to nanostructured photovoltaics. Adv Mater 23:5712–5727
14. Fan ZY, Ruebusch DJ, Rathore AA et al (2009) Challenges and prospects of nanopillar-based solar cells. Nano Res 2:829–843
15. Peng KQ, Lee ST (2011) Silicon nanowires for photovoltaic solar energy conversion. Adv Mater 23:198–215
16. Han N, Wang F, Ho JC (2012) One-dimensional nanostructured materials for solar energy harvesting. Nanomater Energy 1:4–17
17. Kempa TJ, Cahoon JF, Kim SK et al (2012) Coaxial multishell nanowires with high-quality electronic interfaces and tunable optical cavities for ultrathin photovoltaics. Proc Natl Acad Sci USA 109:1407–1412
18. Cao LY, White JS, Park JS et al (2009) Engineering light absorption in semiconductor nanowire devices. Nat Mater 8:643–647
19. Anttu N, Lehmann S, Storm K et al (2014) Crystal phase-dependent nanophotonic resonances in InAs nanowire arrays. Nano Lett 14:5650–5655
20. Heiss M, Morral AFI (2011) Fundamental limits in the external quantum efficiency of single nanowire solar cells. Appl Phys Lett 99:263102
21. Krogstrup P, Jorgensen HI, Heiss M et al (2013) Single-nanowire solar cells beyond the Shockley–Queisser limit. Nat Photonics 7:306–310
22. Xu YL, Gong T, Munday JN (2015) The generalized Shockley–Queisser limit for nanostructured solar cells. Sci Rep 5:13536
23. Anttu N (2015) Shockley–Queisser detailed balance efficiency limit for nanowire solar cells. Acs Photonics 2:446–453
24. Peng KQ, Xu Y, Wu Y et al (2005) Aligned single-crystalline Si nanowire arrays for photovoltaic applications. Small 1:1062–1067
25. Diedenhofen SL, Vecchi G, Algra RE et al (2009) Broad-band and omnidirectional antireflection coatings based on semiconductor nanorods. Adv Mater 21:973–978
26. Muskens OL, Rivas JG, Algra RE et al (2008) Design of light scattering in nanowire materials for photovoltaic applications. Nano Lett 8:2638–2642
27. Garnett E, Yang PD (2010) Light trapping in silicon nanowire solar cells. Nano Lett 10:1082–1087
28. Yan RX, Gargas D, Yang PD (2009) Nanowire photonics. Nat Photonics 3:569–576
29. Lin Q, Hua B, Leung SF et al (2013) Efficient light absorption with integrated nanopillar nanowell arrays for three-dimensional thin-film photovoltaic applications. ACS Nano 7:2725–2732
30. Lin QF, Leung SF, Lu LF et al (2014) Inverted nanocone-based thin film photovoltaics with omni directionally enhanced performance. ACS Nano 8:6484–6490
31. Leung SF, Tsui KH, Lin QF et al (2014) Large scale, flexible and three-dimensional quasi-ordered aluminum nanospikes for thin film photovoltaics with omnidirectional light trapping and optimized electrical design. Energy Environ Sci 7:3611–3616
32. Qiu YC, Leung SF, Zhang QP et al (2015) Nanobowl optical concentrator for efficient light trapping and high-performance organic photovoltaics. Sci Bull 60:109–115
33. Lin H, Xiu F, Fang M et al (2014) Rational design of inverted nanopencil arrays for cost-effective, broadband, and omnidirectional light harvesting. ACS Nano 8:3752–3760
34. Lin H, Cheung HY, Xiu F et al (2013) Developing controllable anisotropic wet etching to achieve silicon nanorods, nanopencils and nanocones for efficient photon trapping. J Mater Chem A 1:9942–9946
35. Diedenhofen SL, Janssen OTA, Grzela G et al (2011) Strong geometrical dependence of the absorption of light in arrays of semiconductor nanowires. ACS Nano 5:2316–2323
36. Fan ZY, Kapadia R, Leu PW et al (2010) Ordered arrays of dual-diameter nanopillars for maximized optical absorption. Nano Lett 10:3823–3827
37. Kelzenberg MD, Boettcher SW, Petykiewicz JA et al (2010) Enhanced absorption and carrier collection in Si wire arrays for photovoltaic applications. Nat Mater 9:239–244
38. Fortuna SA, Li XL (2009) GaAs MESFET with a high-mobility self-assembled planar nanowire channel. IEEE Electron Device Lett 30:593–595
39. Spirkoska D, Arbiol J, Gustafsson A et al (2009) Structural and optical properties of high quality zinc-blende/wurtzite GaAs nanowire heterostructures. Phys Rev B 80:245325
40. Parkinson P, Joyce HJ, Gao Q et al (2009) Carrier lifetime and mobility enhancement in nearly defect-free core-shell nanowires measured using time-resolved terahertz spectroscopy. Nano Lett 9:3349–3353
41. Walukiewicz W, Lagowski J, Jastrzebski L et al (1979) Minority-carrier mobility in P-type GaAs. J Appl Phys 50:5040–5042
42. Perera S, Fickenscher MA, Jackson HE et al (2008) Nearly intrinsic exciton lifetimes in single twin-free GaAs/AlGaAs core-shell nanowire heterostructures. Appl Phys Lett 93:053110
43. Zhang W, Lehmann S, Mergenthaler K et al (2015) Carrier recombination dynamics in sulfur-doped InP nanowires. Nano Lett 15:7238–7244
44. Gutsche C, Niepelt R, Gnauck M et al (2012) Direct determination of minority carrier diffusion lengths at axial GaAs nanowire p-n junctions. Nano Lett 12:1453–1458

45. Lysov A, Vinaji S, Offer M et al (2011) Spatially resolved photoelectric performance of axial GaAs nanowire pn-diodes. Nano Res 4:987–995
46. Thelander C, Caroff P, Plissard S et al (2011) Effects of crystal phase mixing on the electrical properties of InAs nanowires. Nano Lett 11:2424–2429
47. Wallentin J, Ek M, Wallenberg LR et al (2012) Electron trapping in InP nanowire FETs with stacking faults. Nano Lett 12:151–155
48. Joyce HJ, Wong-Leung J, Gao Q et al (2010) Phase perfection in zinc blende and wurtzite III–V nanowires using basic growth parameters. Nano Lett 10:908–915
49. Krogstrup P, Popovitz-Biro R, Johnson E et al (2010) Structural phase control in self-catalyzed growth of GaAs nanowires on silicon (111). Nano Lett 10:4475–4482
50. Joyce HJ, Gao Q, Tan HH et al (2009) Unexpected benefits of rapid growth rate for III–V nanowires. Nano Lett 9:695–701
51. Breuer S, Pfüller C, Flissikowski T et al (2011) Suitability of Au- and self-assisted GaAs nanowires for optoelectronic applications. Nano Lett 11:1276–1279
52. Hemesath ER, Schreiber DK, Gulsoy EB et al (2011) Catalyst incorporation at defects during nanowire growth. Nano Lett 12:167–171
53. Han N, Hou JJ, Wang FY et al (2013) GaAs nanowires: from manipulation of defect formation to controllable electronic transport properties. ACS Nano 7:9138–9146
54. Han N, Wang F, Hou JJ et al (2012) Manipulated growth of GaAs nanowires: controllable crystal quality and growth orientations via a supersaturation-controlled engineering process. Cryst Growth Des 12:6243–6249
55. Zhang Z, Lu ZY, Chen PP et al (2013) Quality of epitaxial InAs nanowires controlled by catalyst size in molecular beam epitaxy. Appl Phys Lett 103:073109
56. O'Regan C, Biswas S, Barth S et al (2014) Size-controlled growth of germanium nanowires from ternary eutectic alloy catalysts. J Mater Chem C 2:4597–4605
57. O'Regan C, Biswas S, O'Kelly C et al (2013) Engineering the growth of germanium nanowires by tuning the supersaturation of Au/Ge binary alloy catalysts. Chem Mater 25:3096–3104
58. Mariani G, Wong PS, Katzenmeyer AM et al (2011) Patterned radial GaAs nanopillar solar cells. Nano Lett 11:2490–2494
59. Kim DR, Lee CH, Rao PM et al (2011) Hybrid Si microwire and planar solar cells: passivation and characterization. Nano Lett 11:2704–2708
60. Tajik N, Peng Z, Kuyanov P et al (2011) Sulfur passivation and contact methods for GaAs nanowire solar cells. Nanotechnology 22:225402
61. Mariani G, Scofield AC, Hung CH et al (2013) GaAs nanopillar-array solar cells employing in situ surface passivation. Nat Commun 4:1497
62. Yang ZX, Han N, Fang M et al (2014) Surfactant-assisted chemical vapour deposition of high-performance small-diameter GaSb nanowires. Nat Commun 5:5249
63. Kelzenberg MD, Turner-Evans DB, Putnam MC et al (2011) High-performance Si microwire photovoltaics. Energy Environ Sci 4:866–871
64. Kempa TJ, Tian BZ, Kim DR et al (2008) Single and tandem axial p-i-n nanowire photovoltaic devices. Nano Lett 8:3456–3460
65. Aashir W, Zhang Q, Tavakoli MM et al (2016) Performance improvement of solution-processed CdS/CdTe solar cells with a thin compact TiO_2 buffer layer. Sci Bull 61:86–91
66. Holm JV, Jorgensen HI, Krogstrup P et al (2013) Surface-passivated GaAsP single-nanowire solar cells exceeding 10% efficiency grown on silicon. Nat Commun 4:1498
67. Wallentin J, Anttu N, Asoli D et al (2013) InP nanowire array solar cells achieving 13.8% efficiency by exceeding the ray optics limit. Science 339:1057–1060
68. Léonard F, Talin AA (2011) Electrical contacts to one-and two-dimensional nanomaterials. Nat Nanotechnol 6:773–783
69. del Alamo JA (2011) Nanometre-scale electronics with III–V compound semiconductors. Nature 479:317–323
70. Li HY, Wunnicke O, Borgström M et al (2007) Remote p-doping of InAs nanowires. Nano Lett 7:1144–1148
71. Han N, Wang F, Yip S et al (2012) GaAs nanowire schottky barrier photovoltaics utilizing Au–Ga alloy catalytic tips. Appl Phys Lett 101:013105
72. Ye Y, Dai Y, Dai L et al (2010) High-performance single CdS nanowire (nanobelt) Schottky junction solar cells with au/graphene Schottky electrodes. ACS Appl Mater Interfaces 2:3406–3410
73. Yang LJ, Wang S, Zeng QS et al (2011) Efficient photovoltage multiplication in carbon nanotubes. Nat Photonics 5:673–677
74. Heurlin M, Wickert P, Falt S et al (2011) Axial InP nanowire tandem junction grown on a silicon substrate. Nano Lett 11:2028–2031
75. Han N, Yang ZX, Wang F et al (2015) High performance GaAs nanowire solar cells for flexible and transparent photovoltaics. ACS Appl Mater Interfaces. doi:10.1021/acsami.1025b06452
76. Kelzenberg MD, Turner-Evans DB, Kayes BM et al (2008) Photovoltaic measurements in single-nanowire silicon solar cells. Nano Lett 8:710–714
77. Tian BZ, Zheng XL, Kempa TJ et al (2007) Coaxial silicon nanowires as solar cells and nanoelectronic power sources. Nature 449:885–890
78. Tang YB, Chen ZH, Song HS et al (2008) Vertically aligned p-type single-crystalline GaN nanorod arrays on n-type Si for heterojunction photovoltaic cells. Nano Lett 8:4191–4195
79. Garnett EC, Yang PD (2008) Silicon nanowire radial p-n junction solar cells. J Am Chem Soc 130:9224–9225
80. Colombo C, Heiss M, Gratzel M et al (2009) Gallium arsenide p-i-n radial structures for photovoltaic applications. Appl Phys Lett 94:173108
81. Tang JY, Huo ZY, Brittman S et al (2011) Solution-processed core-shell nanowires for efficient photovoltaic cells. Nat Nanotechnol 6:568–572
82. Dhaka V, Haggren T, Jussila H et al (2012) High quality GaAs nanowires grown on glass substrates. Nano Lett 12:1912–1918
83. Han N, Wang FY, Hui AT et al (2011) Facile synthesis and growth mechanism of Ni-catalyzed GaAs nanowires on non-crystalline substrates. Nanotechnology 22:285607
84. Colombo C, Krogstrup P, Nygard J et al (2011) Engineering light absorption in single-nanowire solar cells with metal nanoparticles. New J Phys 13:123026
85. Atwater HA, Polman A (2010) Plasmonics for improved photovoltaic devices. Nat Mater 9:205–213
86. Li YH, Yan X, Wu Y et al (2015) Plasmon-enhanced light absorption in GaAs nanowire array solar cells. Nanoscale Res Lett 10:436
87. Wu K, Chen J, McBride JR et al (2015) Efficient hot-electron transfer by a plasmon-induced interfacial charge-transfer transition. Science 349:632–635
88. Clavero C (2014) Plasmon-induced hot-electron generation at nanoparticle/metal-oxide interfaces for photovoltaic and photocatalytic devices. Nat Photonics 8:95–103
89. DuChene JS, Sweeny BC, Johnston-Peck AC et al (2014) Prolonged hot electron dynamics in plasmonic-metal/semiconductor heterostructures with implications for solar photocatalysis. Angew Chem Int Edit 53:7887–7891
90. Davis NJLK, Bohm ML, Tabachnyk M et al (2015) Multiple-exciton generation in lead selenide nanorod solar cells with external quantum efficiencies exceeding 120 %. Nat Commun 6:8259
91. Dorodnyy A, Alarcon-Llado E, Shklover V et al (2015) Efficient multiterminal spectrum splitting via a nanowire array solar cell. ACS Photonics 2:1284–1288
92. Yuhas BD, Yang PD (2009) Nanowire-based all-oxide solar cells. J Am Chem Soc 131:3756–3761
93. Musselman KP, Wisnet A, Iza DC et al (2010) Strong efficiency improvements in ultra-low-cost inorganic nanowire solar cells. Adv Mater 22:E254–E258